The interplay of lithology, tectonics and climate in the morphology of Corsica

Rebekah M. Harries, Chrystiann Lavarini, Linda A. Kirstein, Mikael Attal & Simon M. Mudd

The interplay of lithology, tectonics and climate in the morphology of Corsica

Rebekah M. Harries[a], Chrystiann Lavarini[b], Linda A. Kirstein[b*], Mikael Attal[c], Simon M. Mudd[c]

[a] Institute of Hazard, Risk and Resilience, Durham University Lower Mount Joy, South Rd, Durham DH1 3LE

[b] School of GeoSciences, Grant Institute, University of Edinburgh, Edinburgh, UK, EH9 3FE

[c] School of GeoSciences, University of Edinburgh, Edinburgh, UK, EH8 9XP

Corresponding author *

email: linda.kirstein@ed.ac.uk

Key points:

- Corsica is a transient, segmented and dynamic landscape with strong lithological contrasts

- Tributary height above main stem channel provides a novel approach to documenting disequilibrium

- Knickpoint size and distribution do not reflect specific base-level changes

- Geological structures control valley orientation and knickpoint distribution, even within uniform lithologies

- Conditioning of the landscape by glaciation has long-term impact on drainage evolution

Abstract

The morphology of the landscape on the island of Corsica in the western Mediterranean is transient with clear topographic asymmetry. The geology of the island can be divided into two units – Hercynian Corsica and Alpine Corsica, with contrasting lithology, climate and structural controls between them. Here, topographic analysis is used to assess the influence of each of these factors on landscape form. Disequilibrium in the landscape is illustrated by analysing chi and Gilbert metrics which indicate active drainage divide migration, along with a new metric that quantifies tributary heights above the main stem channel. Climate in the region has fluctuated dramatically from the Messinian salinity crisis through to Quaternary glaciation. However, analysis of the size and distribution of knickpoints across the island does not reflect specific base-level changes. Instead, basement structures control valley orientation and conditioning of the landscape by glaciation exerts strong controls on drainage evolution.

1. Introduction

There is debate regarding the relative controls exerted by lithology, tectonics and climate on the development of topography and on the topographic response to changes in boundary conditions (Whipple, 2001; Mudd, 2017). Studies integrating the analysis of various parts of the landscape offer the best opportunity to disentangle such controls, as river profiles, hillslopes and drainage divides are expected to respond differently to different forcings. For example, river profiles and hillslopes record changes in erosion, exhumation and uplift rates over a range of short to long timescales (10^4 to 10^7 years) (Whipple, 2001; Kirstein et al., 2014; Finnegan et al., 2014; Mudd, 2017). River steepness has been used as a proxy for inferring spatial changes in rock uplift and erodibility, while breaks in channel slope (knickpoints) have been used to infer temporal and spatial changes in erosion in response to varying environmental conditions (e.g., erodibility, structural boundaries, and uplift) (Crosby and Whipple, 2006; Baynes et al., 2015; Brocard et al., 2016). On shorter timescales ($<10^4$ years) different parts of the geomorphic system may be responding to different forcings at different times, e.g., base-level changes coupled with glaciation should result in complex adjustment signals in downstream and upstream catchment areas respectively.

Corsica is an ideal location to study the interplay between tectonics, erosion and climate (Figure 1). The mountainous island has experienced exhumation rates of 25 to 220 mm/kyr since the late Miocene, and erosion rates of similar magnitude over the Quaternary (Fellin et al., 2005; Kuhlemann et al., 2007, 2009; Sømme et al. 2011; Molliex et al., 2017). With a maximum elevation of 2706 m, the high summits of Corsica have experienced glaciation during the last glacial maximum (Kuhlemann et al., 2005) (Figure 2). A precipitation gradient exists across the island (Kuhlemann et al., 2005; Fick and Hijmans, 2017) (Figure 2). Importantly, the bulk of the island is made of a N-S elongated Hercynian basement block (mostly granitoids and associated felsic volcanic rocks) that encompasses the highest summits and the main N-S drainage divide (Figures 1, 3). To the NE, this basement block is flanked by a slab of Alpine units (mostly flysch and ophiolite) (Figure 3) which has the effect of lengthening the eastward draining rivers. Corsica's topography also reveals an asymmetry of the main drainage divide which is located to the west of the central axis of Hercynian Corsica to the north, and to the east of this axis in the south (Figure 1). This curious divide configuration raises questions about its origin, and if it may be caused by temporally variable climate and/or tectonic forcings.

The modern topography of Corsica features lithological variability, precipitation gradients and recent glaciation, all of which are superimposed on an active tectonic legacy. Our aim is to disentangle these factors to understand why the morphology of the northern part of the island is fundamentally different to that of the south of the island. We analyse channel longitudinal profiles, identify breaks in slope (i.e., knickpoints) and quantify topographic proxies for the stability of drainage divides and hillslopes. We also develop a new method that quantifies the elevation difference between tributary sources and main channels to illustrate over-deepening of either tributaries or main stem. Combined, these approaches allow us to test whether transient signals can be identified and to assess the degree of sensitivity of the landscape adapting to external forcing. The insights gained should be applicable to evaluating other high-relief, post-glacial landscapes around the globe.

2. Study Area: Corsica

Corsica is the fourth largest island in the Mediterranean Sea with a number of mountain peaks >2000 m in elevation (Figure 2). East-west, across the island's 83 km width, there

are dramatic total relief changes and large cut–and–fill Quaternary river terraces which indicate landscape transience. From south to north, mountain relief increases, which may be partially related to its tectonic history. In the south, minimum elevation varies from sea-level to ~650 m, while maximum elevation is ~2200 m along the indicative 45 km swath profile (Figure 1). This is in contrast to the north where minimum elevation changes from sea-level to 1100 m, and maximum elevations are >2600 m (Figure 1). The form and location of the drainage divide are distinctly different between the south and the north. The drainage divide is asymmetric and located further east in the south, with noticeably greater elevation (and steeper relief to the east) (Figure 2).

The northeast of the island, known as Alpine Corsica, was accreted during Alpine orogenesis from ~65 to 34 Ma, when oceanic and transitional crust was obducted onto Hercynian Corsica, which makes up the rest of the island (Turco et al., 2012). As a result, there are contrasting lithology and structural controls between Hercynian and Alpine Corsica (Figure 3). The high relief, however, may also be related to lithology, climate gradients and pre-existing geological structures being exploited by river systems.

2.1 Topographic and geological development of the study area

Corsica contains two main geological units; Hercynian and Alpine Corsica (Figures 1, 3). Hercynian Corsica comprises three lithological units that cover the majority of the island's onshore area (Rossi et al., 1994) (Figure 3). These units include unmetamorphosed Carboniferous to Early Permian granitoids, Permian volcanic rocks and gneiss, partly overlain by continental and marine sedimentary rocks (Triassic to Paleocene) and by Eocene foredeep strata that are strongly deformed (Figure 3). The basement fabric with a widely spaced fault pattern determines the SW-NE oriented catchments of western Corsica (Figure 4). Alpine Corsica includes metamorphosed oceanic rocks thrust on top of Eocene foredeep strata and Hercynian basement overlain by Miocene to Pliocene sediments (Figure 3). Thick accumulations of Miocene to Pliocene sediments are located in the east and north-east forming the sedimentary plains of Marama and Aleria (Figure 3).

Corsica experienced protracted exhumation from Mesozoic to Cenozoic times, culminating in the late Miocene following accretion of an Alpine terrain to Hercynian Corsica (Fellin et al., 2005). Apatite fission–track (AFT) and apatite (U–Th)/He (AHe)

dating reveal cooling ages that suggest Cenozoic (40-14 Ma) asymmetric exhumation of Corsica from south to north (Cavazza et al., 2001; Danišík et al., 2007; Fellin et al., 2005; Zarki–Jakni et al., 2004). Exhumation started in the south of Corsica in the Late Oligocene (40–30 Ma) and propagated northward through early Miocene times, reaching the centre at 30–20 Ma, and the northern region at 20–17 Ma (Danišík et al., 2007). The island is considered to be at or approaching exhumational steady–state today (Molliex et al., 2017).

High uplift rates (1.5 km/Myr) are recorded from Middle Miocene (~14 Ma) times, with evidence of drainage reorganisation in the north of Corsica (Cavazza et al., 2007; Fellin et al., 2005b). In the large Golo River watershed (Catchment 3, Figure 3), apatite (U–Th)/He dating provides a long–term exhumation rate of 25 to 220 mm/kyr over the last 7–3 Ma (Fellin et al., 2005b; Kuhlemann et al., 2009).

Published Quaternary erosion rates vary from 15 to 420 mm/kyr (similar to long term estimates) with variability depending on geographic location and applied technique e.g. lower erosion rates are estimated from detrital [10]Be (Kuhlemann et al., 2007, 2009; Sømme et al. 2011; Molliex et al., 2017). Incision rates estimated from river terraces by optically stimulated luminescence (OSL) for the Golo River range from 190 to 420 mm/kyr, with values varying between the different tectonic domains of Hercynian and Alpine Corsica (Sømme et al., 2011). Based on seismic reflection and analysis of offshore basins, Calvès et al. (2013) found catchment–wide erosion rates of 47–219 mm/kyr for the last 130 ka, while Molliex et al. (2017) estimated short–term erosion rates of 15–95 mm/kyr using detrital [10]Be cosmogenic nuclides. In the Tavignano River watershed (Catchment 7, Figure 3), Molliex et al. (2017) measured catchment–wide erosion rates of 40 –74 mm/kyr. These catchment–wide erosion rates are much lower than the incision rates (160 –475 mm/kyr) of the Golo River (Fellin et al. 2005b; Sømme et al. 2011). Although there are no short–term catchment–wide erosion rates available to directly compare both sides of the drainage divide, studies conducted by Kuhlemann et al. (2007, 2009) indicate erosion rates are low at the mountain summits (Kuhlemann et al., 2009). There is a clear spatial variation in the measured erosion rates at the mountain summits in northern Corsica, with a westward increase from 9.1 mm/kyr (east) to 13.6 mm/kyr (centre) to 17.6 mm/kyr (west) (Kuhlemann et al., 2009). These erosion rates correlate with modern annual precipitation rates, which are higher on the western side of the Corsican drainage divide, suggesting a potential climatic influence.

Corsica is located both north and west of active plate boundaries in the Mediterranean region (Figure 1). Seismic activity in the Corsica-Sardinia region is sporadic as indicated by the earthquake catalogue CTPI15 (Rovida et al., 2020). Available GPS measurements in the region indicate that GPS velocity is less than 0.5 mm/year with a weak horizontal velocity field (Devoti et al., 2017). Neotectonic activity in the region is limited.

2.2 Sea Level and Climate

Corsica's position in the western Mediterranean Sea means it retains an excellent record of climate change since the Pliocene. The Messinian crisis affected the Mediterranean region during the late Miocene (Gargani, 2004). The first phase of drying out ~5.9 Myr, lasted ~ 400 kyr, and resulted in 600 –700 m of sea level fall at an average rate of ~ 1.45 mm/yr. The second phase of drying out ~ 5.5 Ma was marked by 1300 –1700 m sea level drop over 50 kyr (i.e., 30 mm/yr). The crisis ended around 5.3 Ma (Gargani, 2004). More modest, yet significant sea level variations occurred over the Quaternary, associated with successive glacial and interglacial periods. Waelbroeck et al. (2002) proposed that, in the last 130 ka, Mediterranean Sea level experienced a steady lowering of 120 m between 130–20 ka (i.e., 1.1 mm/yr), followed by a rise to the present level at a rate of ~6 mm/yr. Changes in base-level should, in theory, propagate upstream in drainage networks resulting in transient knickpoint development. The rate at which this occurs is expected to depend on rock strength (e.g. Niemann et al., 2001; Zondervan et al., 2020), however given calc-alkaline granites dominate Hercynian Corsica (Figure 3) differences in rock strength should be minimal.

In the Quaternary, the southern region of the island experienced periglacial activity and glaciers were absent. The northern and central mountains of Hercynian Corsica were strongly glaciated during the Würmian which ended 11,700 years ago, while Alpine Corsica was unglaciated (Kuhlemann et al., 2005) (Figure 2). Glaciers reached their maximum extent ~18 ka ago in the centre and north–western sections of Corsica, extending down to 500 m a.s.l. (Kuhlemann et al., 2005). Remnants of this extensive glaciation include over-deepened valleys, glacial lakes and cirques, which can be made out in the hillshade in Figure 1. Today Corsica is free of permanent ice and experiences a subtropic Mediterranean climate with temperate wet winters and warm, dry summers. Mean annual rainfall varies from ~439 mm in the south to 1061 mm in the northwest (Figure 2). The northeastern parts of the mountain range are drier than the central and southern parts resulting in an asymmetric precipitation pattern (Figure 2). The current

drainage divide is located within the region of the north that was most affected by glaciation (Figure 2).

Here we explore the stability of the Corsica drainage divide and argue that the landscape has been pre-conditioned both by early tectonic activity (fault development) in the south and climate (glacial over-deepening) in the north leading to the migration of the drainage divide to the west in the south and to the east in the north.

3. Methods

To analyse the geomorphology of our study area, we deploy a number of topographic metrics designed to identify areas of heterogeneity in erosion rates or lithology, as well as metrics thought to indicate the stability of the drainage divide. Gilbert (1877) reasoned that steeper channels should erode faster than gentle ones, all else being equal, but a confounding factor is that channel gradient is strongly correlated with drainage area (Morisawa, 1962). Building on Morisawa's (1962) work, Flint (1974) formalized a power law relationship between gradient and drainage area:

$$S = k_s A^{-\theta} \tag{1}$$

where the parameter k_s is defined as the steepness index, and θ is defined as the concavity index. Subsequent work has shown that the steepness index correlates closely with erosion rates (e.g., Kirby and Whipple, 2012; Harel et al. 2016). To calculate k_s we first transform the channel profile by integrating drainage area along the channel (e.g., Perron and Royden, 2013):

$$\chi = \int_{x_b}^{x} \left(\frac{A_0}{A(x)}\right)^{\theta} dx \tag{2}$$

where χ is a longitudinal coordinate in units of meters, A_0 is an arbitrary scaling drainage area, and $z_{(b)}$ is the elevation where integration starts. When $A_0 = 1$ m^2, the gradient $dz/d\chi$ is equal to the steepness index k_s (e.g., Goren et al., 2014; Mudd et al, 2014).

Both the coordinate χ and the steepness index, k_s, depend on the value of the concavity index, θ. To make comparisons between different basins, a reference value of the concavity index, θ_{ref}, is frequently used (Wobus et al., 2006a). Once applied, the steepness indices derived using this reference concavity are referred to as the normalized steepness index, k_{sn}.

Various methods have been proposed to calculate the most likely value of θ for a given drainage basin, but Mudd et al. (2018) found that a method based on the relative disorder of χ-elevation profiles (Hergarten et al. 2016, Goren et al., 2014) was most resilient to tectonic and lithological heterogeneity. After performing a disorder analysis, we selected a θ_{ref} value of 0.35.

We investigate the N–S regional drainage divide of Corsica using both χ and 'Gilbert' metric analyses. Willett et al (2014) proposed differences in χ across divides were indicators of divide migration, with divides moving away from the side with lower values of χ. However, the choice of base–level for the integration, as well as spatial variations in erodibility, Hack's coefficient and channel tortuosity, can significantly affect the χ values of rivers at divides (Whipple et al., 2017; Forte and Whipple, 2018, Gailleton et al., 2021, Zhou et al., 2022a, b) so coupling χ analyses with 'Gilbert metrics' is thought to be more robust. 'Gilbert metrics' represent a top–down assessment of landscape stability, similar to the analysis of "channel-head segments" and the "cross-divide contrast index (C)" recently developed by Zhou et al. which also offers the possibility of identifying uplift gradients and calculating drainage divide migration rates (Zhou et al., 2022a, 2022b, 2024, Zhou and Tan, 2023). Morphometric parameters including upstream gradient, relief and elevation at the channel heads are expected to vary with short–term erosion rates (10^3–10^5 year) and therefore indicate disequilibrium, as suggested by Gilbert (1877) (Forte and Whipple, 2018).

We have used SRTM topographic data with a pixel size of about 30 m, and we set a threshold for initiating a channel at 2500 pixels (corresponding to a drainage area of >2.25 km^2). We then calculated the channel gradient at these source points, averaged over a 10 m drop in elevation as suggested by Wobus et al. (2006a), and compared the difference in the gradient across the divide. The gradient asymmetry across the divide is one of the four "Gilbert metrics" described by Forte and Whipple (2018), although we note that in Forte and Whipple (2018) the gradient is averaged from the channel head to the divide. We prefer using the gradient local to the channel head as the gradient from the channel head to the divide can be sensitive to the hillslope length (e.g., Grieve et al., 2016). Steeper gradients at the same drainage area (in this case the drainage area at fixed number of pixels) should result in faster erosion, all else equal, so the divide should migrate away from the steeper channel.

We located knickpoints along the channel networks. Knickpoints are local steepenings in channel profiles, identified by changes in k_{sn}. These features could be related to changes in underlying channel erodibility (e.g., Duvall et al., 2004), or could be indicative of a change in erosion rate (e.g., Knopf, 1924). Knickpoints that originate from base level changes (e.g., changes to sea level) or differential changes in uplift rates (e.g., from increased fault activity) will migrate upstream (e.g., Knopf, 1924). Royden and Perron (2013) demonstrated that knickpoints originating from a common base level across a landscape with homogenous uplift and substrate should share the same χ coordinate.

We obtain the locations of all knickpoints in our study area by first segmenting the channel network into reaches with similar gradients in χ-elevation space using the statistical method of Mudd et al. (2014). This results in data about this gradient (which is equal to k_{sn}) as a function of χ, and we follow the method of Gailleton et al. (2019) to first denoise the data, combine nearby knickpoints, and then select the largest knickpoints as judged by the change in the channel steepness index. The "magnitude" of the knickpoint is defined by the change in k_{sn} (or Δk_{sn}) across the knickpoint. Denoising is performed on the along channel k_{sn} values using a total variation denoising filter (TVD, Condat, 2013), with a parameter that controls the amount of denoising, l, that has been tuned to the concavity index based on the sensitivity analysis of Gailleton et al., (2019) knickpoints are combined if they are within 10 pixels of each other (i.e. two knickpoints with the same Δk_{sn} within a 10 pixel window will lead to a combined knickpoint double the value of Δk_{sn} compared to one of the original knickpoints). We then thin the dataset (because there are many small changes in k_{sn}) by retaining the largest (by magnitude) 20% of knickpoints. We plot knickpoint locations in conjunction with lithology of the channel bed to differentiate between knickpoints generated by lithological contrasts from those that cannot be explained by lithology (Figure 3).

Finally, we introduce a new metric designed to highlight the presence of hanging tributaries. Hanging tributaries are frequently found in glaciated landscapes and are thought to be caused by differential erosion by glaciers in the main valley and tributaries (e.g., Penck, 1905). Hanging valleys may also be caused by incision in the main channel that exceeds an erosion threshold in tributaries (e.g., Wobus et al., 2006b). In the former case, hanging valleys will be limited to glaciated parts of the landscape, whereas in the latter, hanging valleys will be located downstream of major incision pulses (i.e., downstream of knickpoints). Lithological variations may also lead to hanging valleys, for

example in a situation where a main stem channel exploits a weak lithology; such a situation should lead to patterns of tributary heights above main stem that are distinct from the scenarios presented above. In a landscape without hanging valleys, tributaries at the same χ coordinate as the main stem channel should share the same elevation (Royden and Perron, 2013). A hanging valley, therefore, will have a higher elevation than the main stem channel at the same χ coordinate. We reason that this difference will be most easy to identify at the tributary sources, since those will be upstream of the hanging section, if one exists. We therefore extract the χ coordinate of all tributary sources, and compare the elevation of these sources to the elevation of the main stem channel at the same χ coordinate. We note this metric will be highly sensitive to the θ_{ref} value used in the analysis, which is a limitation. We highlight the importance of using a θ_{ref} value that minimizes the relative disorder of χ-elevation profiles rather than maximizes the linearity of profiles, as such a method was shown to perform best when recovering the θ_{ref} value from simulated topographies in landscapes with non-uniform lithologies and uplift (Mudd et al., 2018).

4. Results

3.1 Drainage divide stability

The regional drainage divide is segmented in two parts (A and B) where a distinct contrast is observed in both χ and the 'Gilbert' gradient metric (Figure 5). The southern section of the Corsica drainage divide (*A*) is marked by values of χ and differences in channel gradient that suggest a westward divide migration trend (i.e., the eastward flowing rivers have lower χ and higher gradient and relief values closer to the divide than the westward ones) (Figure 5, Supplementary Figure 1). However, the northern section of the drainage divide (B) highlights an eastward divide migration trend (i.e., the westward flowing rivers have lower χ and higher gradient and relief values closer to the divide than the eastward ones) (Figure 5, Supplementary Figure 1).

3.2 Spatial distribution and dimensions of knickpoints

The occurrence of knickpoints shows an interesting spatial distribution with respect to tectonic structures and the extent of Würmian glaciation (Figure 3, 4). Migrating knickpoints can be generated by base level changes or differential uplift at faults. Base level changes derived from changing sea level would result in clustering of knickpoints at similar χ locations in channels with similar substrates (e.g., Royden and Perron, 2013).

We observe no such clustering. This suggests that any response to Pliocene-Pleistocene base level change, if it were once present, has migrated through the system or dissipated (Figure 3).

A widely spaced NE-SW Hercynian fault pattern determines the form of many of the catchments and the orientation of many of the rivers of western Corsica (Figure 4). However, despite the prevalence of these faults in Hercynian Corsica, the majority of large knickpoints are located north of 465000 (Figure 3). South of 465000, the largest knickpoints occur in the headwaters of catchments where major faults are present and appear to be exploited by the river. Lithology mapped at the scale provided in Figure 3 does not seem to play an important role in dictating knickpoint location.

3.3 Tributary height above mainstem

Using the novel approach of calculating the difference in height between the main stem channel and the associated tributaries, we find large elevation differences across the island in tributary height as compared to equivalent height, at the same χ location, in the main stem channel (Figure 4). Some of the tributaries, particularly in Alpine Corsica, have accumulated sediment fill (Figure 3), and channels are below the main channel at the same χ coordinate (Figure 4). Tributaries in the northern regions that experienced extensive glaciation in the Würmian are perched high (~200 to 500 m) above the main channel in the region affected by the last glacial maximum (Figure 4). Many of the NE-SW oriented channels south of northing 465000 show high elevation tributaries to the south of the main stem which are fault controlled e.g. catchment 15 (Figure 4).

We also calculated tributary differences using chi Q (Supplementary Figure 2) to try to isolate the extent to which the differences might be explainable by precipitation gradients alone. There is no noticeable difference between the results.

5. Discussion

Our analysis of a range of topographic metrics and their relationship with lithological units, tectonic structures and climate suggests that the topographic state of Corsica is transient and adjusting. The current drainage divide is highly asymmetric, located to the west in the north and to the east in the south (Figure 2).

We deployed the Gilbert gradient metric and the difference in the χ coordinate across the divide to assess the stability of the drainage divide. Two of the recommended uncertainty monitors (i.e. 1 standard error, 95% bootstrap confidence interval and *t*–tests) reveal a

statistically significant migration trend in Corsica (Supplementary Figure 1). The Gilbert and χ metrics show the same migration direction (westward in the southern drainage divide and eastward in the northern drainage divide) which suggests that Corsica is undergoing a horizontal rearrangement of its drainage network and is not in steady–state. It also suggests that the disequilibrium is strong: while Gilbert metrics are expected to reflect the dynamics of drainage divides by focusing on differences in topography near the divide, the χ value has been shown to be highly sensitive to lithological variations and tectonic discontinuities along river profiles (Whipple et al., 2017; Forte and Whipple, 2018, Gailleton et al., 2021, Zhou et al., 2022a, b), which abound in Corsica. Yet, Gilbert metrics and χ disequilibrium at divides agree on a regional scale (Figure 5). The absence of obvious recent discrete river captures suggests that drainage expansion has happened primarily by continuous area gain/loss since the Pliocene, when the last discrete river captures are recorded in the north–east of Corsica (Daníšík et al., 2012; Fellin et al., 2005).

Knickpoints associated with transient signals should, by definition, separate a relict upstream area from a downstream region through which a wave of incision has propagated (Bishop et al., 2005; Crosby and Whipple, 2006). The largest knickpoints in Corsica appear unrelated to sea-level or base-level changes, i.e., they do not occur at a constant χ distance from the coastline even where lithology is constant (Figure 3). Instead, the largest knickpoints are clustered in the north-west, in the region most affected by Würmian glaciation (Figure 2, 3). Given the absence of neotectonic activity on Corsica we make a simple calculation of the adjustment timescale of the landscape. Mitchell and Yanites (2019), using a modified version of the analysis of Royden and Perron (2013), showed that the location of a migrating knickpoint in χ-space is simply $\chi_{kp} = K\,t$, where K is an erodibility coefficient and t is the time elapsed from the originating time of the knickpoint, if the slope exponent is assumed to be unity. The erodibility, K, can be estimated by dividing the erosion rate by k_{sn} (again assuming the slope exponent is unity). Note that in this calculation the same value of θ_{ref} needs to be used for both calculation of χ and k_{sn}. The values of k_{sn} over the channel networks are on the order of 20 (Figure 3), and for erosion rates of 100 mm/kyr (on the slower end of erosion rate estimates since 7 Ma) we calculate knickpoints migrating 5 m in χ space every 1 million years. This slowing of erosion rates in the mid-Miocene could therefore be linked to profile concavities (e.g., in catchments 13 and 17, Figure 3), but again these changes to the

channel steepness are not present in all catchments, and cannot explain hanging valleys that occur at much shorter χ distances. Early differential tectonic activity has therefore no clear impact on the location of knickpoints in either Hercynian or Alpine Corsica. Drainage organization and planform morphology are strongly impacted by rainfall patterns (Han et al., 2015). In Corsica, mean annual rainfall is asymmetric with the highest rainfall related to regions of high relief (Figure 2). This high precipitation is located over the expanding side of the drainage divide, potentially resulting in a top–down wave of erosion that is independent of headward knickpoint propagation. In the north, the situation is complicated by glacial pre-conditioning of the landscape with over-deepened valleys as is evident from the tributary – mainstem channel elevation difference (Figure 4). Alpine Corsica is characterised by very few large knickpoints except at the boundary with Hercynian Corsica. Given the known fluctuations in sea-level in the Mediterranean during the Pliocene and Pleistocene, this may be indicative of rapid diffusion and equilibration of the channel profile within these primarily sedimentary (proto)lithologies. Lithology is therefore considered to be a third order variable in knickpoint development in Corsica. However, geological structures are significant as linear zones of weakness that create local contrasts in erosional efficiency. For example, many of the large knickpoints in catchment 15 align in a NE-SW direction on the south side of the trunk stream (Figure 3, 4) which we interpret as the result of the drainage network exploiting the NE-SW basement fracture pattern inherited from the Hercynian orogeny. This shows the importance of local structures on landscape morphology, even in locations with apparent lithological homogeneity (Figure 4). Our knowledge of the strong NE-SW fabric across Hercynian Corsica allows us to identify the source of the documented knickpoints in catchment 15. Without this geological knowledge, these knickpoints, which occur within a uniform lithology, could have been interpreted as evidence of neotectonics.

The impact of climate on the landscape is clear. The topography in the north-west was substantively affected by Pleistocene glaciation over-deepening valleys and perching tributaries. This combination of early tectonic activity which led to the growth of the mountainous landscape of Corsica and climate change appears to be driving the transient, mobile form of the landscape evident today. Note that while tectonics can set signals in motion that may lead to drainage divide disequilibrium long after cessation of uplift (e.g., an asymmetric drainage divide may move towards a more central position in a mountain range in response to the cessation of an uplift gradient), we do not believe that tectonics

alone could explain the topography of Corsica, and in particular the contrast between the two sections of the drainage divide, in the absence of a major tectonic discontinuity at the transition between these two sections.

6. Conclusion

Based on the statistical analyses of 'Gilbert' and χ metrics, two major directions of drainage divide migration were identified in Corsica. The northern section of the drainage divide is currently migrating to the east, while the southern section is migrating westward. These patterns suggest that Corsica is in a transient state. The current direction of drainage divide motion mirrors the predicted trend required to ultimately reach a horizontal steady–state and drainage symmetry.

Hercynian Corsica has a higher density of knickpoints especially in the region that experienced permanent glaciation in the Würmian (Figure 2). Tributaries in the region are perched high above the main channel stem (Figure 4). The modern drainage divide in the north is currently located in the region where glaciation was extensive and valleys are over-deepened. Mean annual precipitation is highest east of the drainage divide in northern Corsica and indicates the direction that the divide is expanding towards.

The combination of tectonic and climatic pre-conditioning of the landscape has markedly influenced the form of the channel network and the topographic response in Corsica. A similar control may be evident elsewhere in regions that are devoid of strong tectonic signals (e.g., tectonically quiescent) but have experienced climate changes.

7. Acknowledgements

8. References

Baynes, E.R.C., Attal, M., Dugmore, A.J., Kirstein, L.A., Whaler, K.A., 2015. Catastrophic impact of extreme flood events on the morphology and evolution of the lower Jökulsá á Fjöllum (northeast Iceland) during the Holocene: Geomorphology 250: 422-436.

Bishop, P. and Hoey, T. B. and Jansen, J. D. and Artza, I. L. 2005. Knickpoint recession rate and catchment area: the case of uplifted rivers in Eastern Scotland. Earth Surface Processes and Landforms 30(6): 767-778.

Brocard, G.Y., Willenbring, J.K., Miller, T.E., Scatena, F.N., 2016. Relict landscape resistance to dissection by upstream migrating knickpoints: Journal of Geophysical Research: Earth Surface 121 (6): 1182-1203.

Calvès G, Toucanne S, Jouet G, Charrier S, Thereau E, Etoubleau J, Marsset T, Droz L, Bez M, Jorry S, Mulder T, Lericolais G. 2013. Inferring denudation variations from the sediment record; an example of the last glacial cycle record of the Golo basin and watershed, East Corsica, Western Mediterranean Sea. Basin Research 24: 1–22.

Cavazza W, Zattin M, Ventura B, Zuffa GG. 2001. Apatite fission– track analysis of Neogene exhumation in northern Corsica (France). Terra Nova 13: 51–57.

Cavazza, W., DeCelles, P. G., Fellin, M. G., Paganelli, L. 2007. The Miocene Saint–Florent Basin in northern Corsica: stratigraphy, sedimentology, and tectonic implications. Basin Research 19(4), 507– 527.

Condat, L., 2013. A Direct Algorithm for 1D Total Variation Denoising. IEEE SIGNAL PROC. LETTERS 20, 1054–1057. https://doi.org/10.1109/LSP.2013.2278339

Crosby, B. T., and Whipple, K.X., 2006. Knickpoint initiation and distribution within fluvial networks: 236 waterfalls in the Waipaoa River, North Island, New Zealand, Geomorphology, 82, 16– 38, doi:10.1016/j.geomorph.2005.1008.1023.

Daníšík M, Kuhlemann J, Dunkl I, Evans NJ, Székely B, Frisch W. 2012. Survival of ancient landforms in a collisional setting as revealed by combined fission track and (U–Th)/He thermochronometry: a case study from Corsica (France). Journal of Geology 120(2): 155–173.

Devoti, R., D'Agostino, N., Serpelloni, E., Pietrantonio, G., Riguzzi, F., Avallone, A., Cavaliere, A., Cheloni, D., Cecere, G., D'Ambrosio, C., Franco, L., Selvaggi, G., Metois, M., Esposito, A., Sepe, V., Galvani, A., Anzidei, M. 2017. A Combined Velocity Field of the Mediterranean Region. Annals of Geophysics, 60(2), S0215. doi: 10.4401/ag-7059.

Duvall, A., Kirby, E., Burbank, D., 2004. Tectonic and lithologic controls on bedrock channel profiles and processes in coastal California. Journal of Geophysical Research: Earth Surface 109, doi:10.1029/2003JF000086.

Fellin MG, Picotti V, Zattin M. 2005. Neogene to Quaternary rifting and inversion in Corsica: retreat and collision in the western Mediterranean. Tectonics 24: doi: 10.1029/2003TC001613.TC1011.

Fellin MG, Zattin M, Picotti V, Reiners PW, Nicolescu S. 2005b. Relief evolution in northern Corsica (western Mediterranean): Constraints on uplift and erosion on long–term and short– term timescales. Journal of Geophysical Research 110, doi:10.1029/2004JF000167.F01016.

Fick, S.E., R.J. Hijmans, 2017. WorldClim 2: new 1km spatial resolution climate surfaces for global land areas. International Journal of Climatology 37 (12): 4302-4315.

Finnegan, N.J., Schumer, R., and Finnegan, S., 2014. A signature of transience in rates of river incision into bedrock over timescales of 10^4-10^7 years, Nature 505, 391-394.

Flint, J.J., 1974. Stream gradient as a function of order, magnitude, and discharge. Water Resources Research 10, 969–973, doi.org/10.1029/WR010i005p00969.

Forte, A.M. Whipple, K.X., 2018. Criteria and tools for determining drainage divide stability: Earth and Planetary Science Letters 493, 102-117, doi: 10.1016/j.epsl.2018.04.026.

Gargani, J. 2004. Modelling of the erosion in the Rhone valley during the Messinian crisis (France). Quaternary International 121(1), 13– 22.

Gilbert, G. K. 1877. Report on the Geology of the Henry Mountains. US Government Printing Office.

Grieve, S.W.D., Mudd, S.M., Hurst, M.D., 2016. How long is a hillslope? Earth Surface Processes and Landforms 41, 1039–1054. https://doi.org/10.1002/esp.3884

Hu, K., Fang, X., Ferrier, K.L., Granger, D.E., Zhao, Z., Ruetenik, G.A., 2021. Covariation of cross-divide differences in denudation rate and χ: Implications for drainage basin reorganization in the Qilian Shan, northeast Tibet. Earth and Planetary Science Letters 562, 116812, doi:10.1016/j.epsl.2021.116812

Kirstein, L.A., Carter, A., Chen, Y-G., 2014. Impacts of arc collision on small orogens: new insights from the Coastal Range detrital record, Taiwan Journal of the Geological Society, London 171, 5–8. doi: 10.1144/jgs2013-046.

Kuhlemann J, Frisch W, Székely B, Dunkl I, Daníšík M, Krumrei I. 2005. Würmian maximum glaciation in Corsica: glacier extent, amplifying paleorelief, and mesoscale climate. Austrian Journal of Earth Science 97: 68–81.

Kuhlemann J, Krumrei I, Daníšík M, Van der Borg K. 2009. Weathering of granite and granitic regolith in Corsica: short– term [10]Be versus long– term thermochronological constraints. *In* Thermochronological Methods: From Palaeotemperature Constraints to Landscape Evolution Models, Lisker F, Ventura B, Glasmacher UA (eds), Geological Society of London Special Publication 324, 217–235.

Kuhlemann J, Van der Borg K, Daníšík M, Frisch W. 2007. In situ [10]Be– erosion rates in granites of subalpine Miocene paleosurfaces in the western Mediterranean (Corsica, France). International Journal of Earth Science 97, 549–564.

Mitchell, N.A., Yanites, B.J., 2019. Spatially Variable Increase in Rock Uplift in the Northern U.S. Cordillera Recorded in the Distribution of River Knickpoints and Incision Depths. Journal of Geophysical Research: Earth Surface 124, 1238–1260. https://doi.org/10.1029/2018JF004880

Molliex, S., Jouet, G., Freslon, N., Bourlès, D. L., Authemayou, C., Moreau, J., Rabineau, M. 2017. Controls on Holocene denudation rates in mountainous environments under Mediterranean climate. Earth Surface Processes and Landforms, 42(2), 272– 289.

Morisawa, M.E. 1962. Quantitative Geomorphology of Some Watersheds in the Appalachian Plateau. Geological Society of America Bulletin 73, 1025–1046, doi: 10.1130/0016-7606.

Mudd, S. M. 2017. Detection of transience in eroding landscapes. Earth Surface Processes and Landforms 42(1), 24– 41.

Niemann, J. D., Gasparini, N. M., Tucker, G. E., Bras, R. L. 2001. A quantitative evaluation of Playfair's law and its use in testing long-term stream erosion models. Earth Surface Processes and Landforms 26(12), 1317-1332. https://doi.org/10.1002/esp.272

Ouimet, W., Whipple, K., Royden, L., Zhiming, S., and Chen, Z. 2007. The influence of large landslides on river incision in a transient landscape: Eastern margin of the Tibetan plateau (Sichuan, China): Geological Society of America Bulletin 119 (11/12), 1462–1476, doi: 10.1130/B26136.1.

Penck, A. 1905. Glacial Features in the Surface of the Alps. The Journal of Geology 13, 1–19.

Perron, J.T., Royden, L. 2013. An integral approach to bedrock river profile analysis. Earth Surface Processes and Landforms, 38, 570-576. https://doi.org/10.1002/esp.3302

Platt, J.P. (2007) From orogenic hinterlands to Mediterranean-style back-arc basins: a comparative analysis. Journal of the Geological Society, 164, 297-311, https://doi.org/10.1144/0016-76492006-093

Royden, L., Perron, J.T. 2013. Solutions of the stream power equation and application to the evolution of river longitudinal profiles. Journal of Geophysical Research: Earth Surface 118, 497–518, doi:10.1002/jgrf.20031.

Rovida A, Locati M, Camassi R, Lolli B, Gasperini P (2020) The Italian earthquake catalogue CPTI15. Bull Earthq Eng. https://doi.org/10.1007/s10518-020-00818-y

Sømme, T. O., Piper, D. J., Deptuck, M. E., & Helland– Hansen, W. 2011. Linking onshore–offshore sediment dispersal in the Golo source– to– sink system (Corsica, France) during the late Quaternary. Journal of Sedimentary Research 81(2), 118– 137.

Turco E., Macchiavelli C., Mazzoli, S., Schettino, A., Pierantoni P. 2012. Kinematic evolution of Alpine Corsica in the framework of Mediterranean mountain belts: Tectonophysics 579, 193-206.

Waelbroeck, C., Labeyrie, L., Michel, E., Duplessy, J. C., McManus, J. F., Lambeck, K., Labracherie, M. (2002). Sea– level and deep water temperature changes derived from benthic foraminifera isotopic records. Quaternary Science Reviews, 21(1– 3), 295– 305.

Whipple, K.X., 2001. Fluvial Landscape Response Time: How Plausible Is Steady-State Denudation? American Journal of Science, 301, 313–325. doi: 10.2475/ajs.301.4-5.313.

Whipple, K. X., DiBiase, R. A., Ouimet, W. B., & Forte, A. M. 2017. Preservation or piracy: Diagnosing low– relief, high– elevation surface formation mechanisms. Geology 45(1), 91– 94.

Willenbring, J.K. Codilean, A.T., McElroy, B. 2013. Earth is (mostly) flat: Apportionment of the flux of continental sediment over millennial time scales. Geology 41 (3), 343–346. doi: https://doi.org/10.1130/G33918.1

Willett, S. D., McCoy, S. W., Perron, J. T., Goren, L., & Chen, C. Y. 2014. Dynamic reorganization of river basins. Science, 343(6175), 1248765.

Wobus, C.W., Whipple, K.X., Kirby, E., Snyder, N., Johnson, J., Spyropolou, K., Crosby, B., Sheehan, D. 2006. Tectonics from topography: Procedures, promise, and pitfalls, in: Special Paper 398: Tectonics, Climate, and Landscape Evolution. Geological Society of America, 55–74. https://doi.org/10.1130/2006.2398(04)

Wobus, C.W., Crosby, B.T., Whipple, K.X. 2006b. Hanging valleys in fluvial systems: Controls on occurrence and implications for landscape evolution. Journal of Geophysical Research: Earth Surface 111. https://doi.org/10.1029/2005JF000406

Young, H.H., Hilley, G.E. 2018. Millennial-scale denudation rates of the Santa Lucia Mountains, California: Implications for landscape evolution in steep, high-relief, coastal mountain ranges. GSA Bulletin 130, 1809–1824. https://doi.org/10.1130/B31907.1

Zhou, C., Tan, X., Liu, Y., Lu, R., Murphy, M. A., He, H., Han, Z., Xu, X. 2022a. Ongoing westward migration of drainage divides in eastern Tibet, quantified from topographic analysis, Geomorphology, 402, 108123, https://doi.org/10.1016/j.geomorph.2022.108123.

Zhou, C., Tan, X., Liu, Y., Shi, F. 2022b. A cross-divide contrast index (C) for assessing controls on the main drainage divide stability of a mountain belt, Geomorphology, 398, 108071, https://doi.org/10.1016/j.geomorph.2021.108071.

Zhou, C., Tan, X. 2023. Quantifying the influence of asymmetric uplift, base level elevation, and erodibility on cross-divide difference, Geomorphology, 427, 108634, https://doi.org/10.1016/j.geomorph.2023.108634.

Zhou, C., Tan, X., Liu, Y., Shi, F. 2024. Quantifying the migration rate of drainage divides from high-resolution topographic data. Earth Surface Dynamics, 12, 433–448, https://doi.org/10.5194/esurf-12-433-2024.

Zondervan, J.R., Stokes, M., Boulton, S.J., Telfer, M.W., Mather, A.E. 2020. Rock strength and structural controls on fluvial erodibility: Implications for drainage divide

mobility in a collisional mountain belt. Earth and Planetary Science Letters, 538, 116221. https://doi.org/10.1016/j.epsl.2020.116221

Figure 1. a. Location of Corsica within the Western Mediterranean domain. Adapted from Pratt, 2007. b. Hillshade of Corsica highlighting two swath profiles (c. and d.) from the northern and southern sections of Hercynian Corsica. The lower line on the swath profile is the minimum elevation within the swath, and roughly tracks the channel elevation. This is used to delineate the drainage divide. The dark blue line is the median elevation, the green area brackets the 25th and 75th percentiles of elevation, and the top line is the maximum elevation in the swath.

Figure 2. (Left) Spatial distribution of mean annual rainfall across Corsica derived from Worldclim climate data for the period 1970-2000 (Fick and Hijmans, 2017). The dotted white line is the glacier extent at the last glacial maximum (after Kuhlemann et al., 2005). (Right) Elevation variation on Corsica colour coded for 500 m intervals. Notice higher elevation is focused to the west in northern Corsica.

Figure 3. Overview of the basic geology of Corsica, the form of the main stem and contributing tributaries for each catchment (labelled 0 to 20), and the location and magnitude of knickpoints (white circles). PDF is "Probability Density Function", with histograms showing the relative abundance of knickpoints per 200 m elevation interval. Knickpoint magnitude is divided by 30 in order to visualise effectively at map scale.

Figure 4. Difference in elevation of tributaries and their main channels at the same chi distance upstream. On the left, the chi-elevation profiles of three catchments located on the eastern (catchments 3 and 7) and western (catchment 15) sides of the drainage divide are presented. Each tributary's source point is coloured according to its elevation above the main channel in chi space. On the right, the tributary sources are plotted in plan-view on top of Corsica's river network. The glacier extent at the last glacial maximum and mapped faults are also included to give tectonic and glacial context.

Figure 5. χ values (left) and normalised values of upstream gradient (right) of the drainage network across Corsica. The regional drainage divide was segmented into two shorter ones (A (south) and B (north)) based on the visual anomaly in χ and gradient. The drainage divide is expected to migrate towards the part with the greatest χ value and channel head elevation, and lowest gradient and relief. As indicated in the lower panel of drainage divide stability metrics, drainage divide A is expected to migrate westwards, while drainage divide B is expected to migrate eastwards. Frequency bars and uncertainty plots in red represent eastward flowing river catchments, while those in blue represent westward flowing river catchments. Mean (μ) and standard deviation (σ) of the channel heads metrics are also coloured accordingly. Error bars represent 1 standard deviation, 95% bootstrap confidence interval and 1 standard error (from top to bottom).
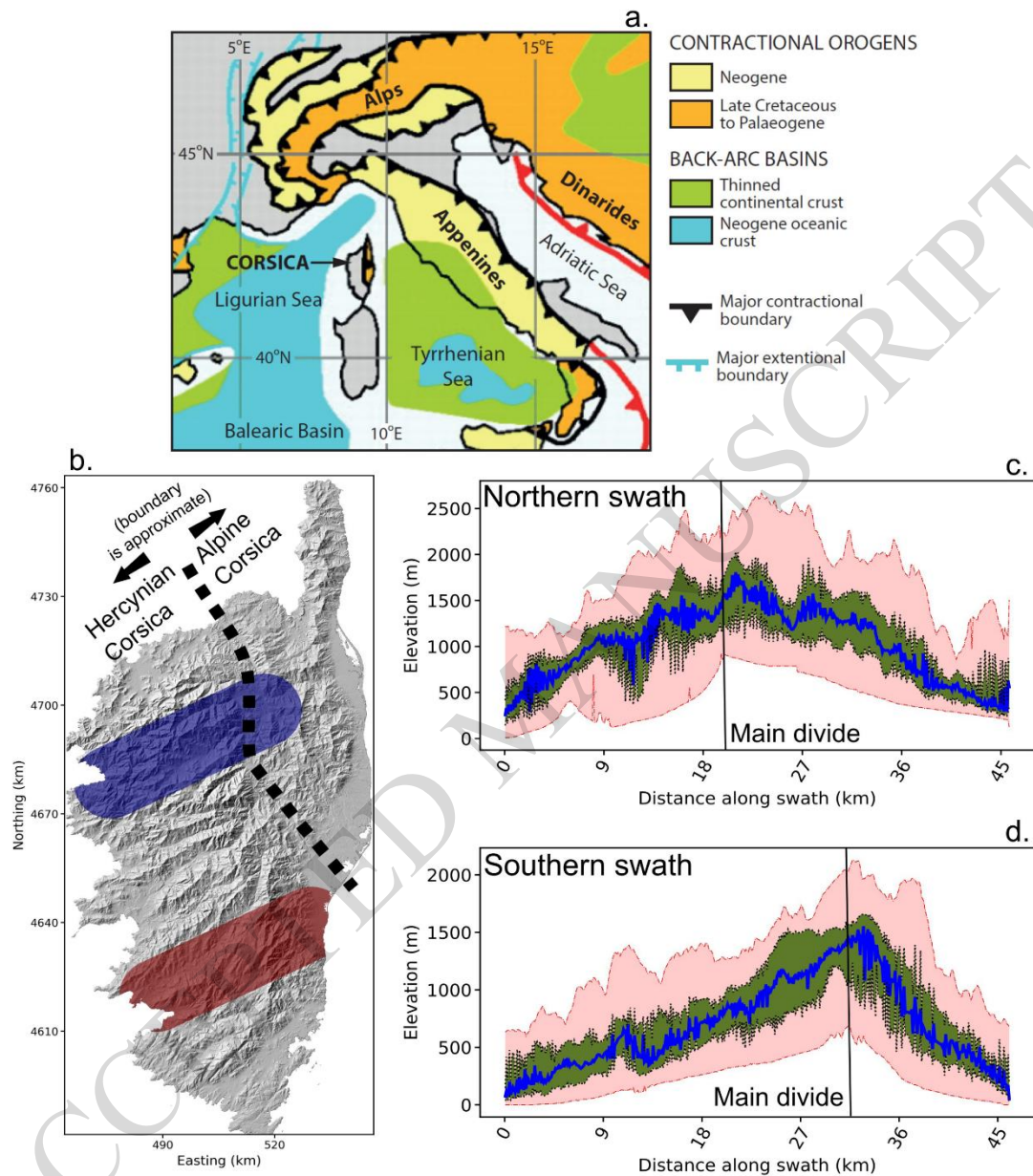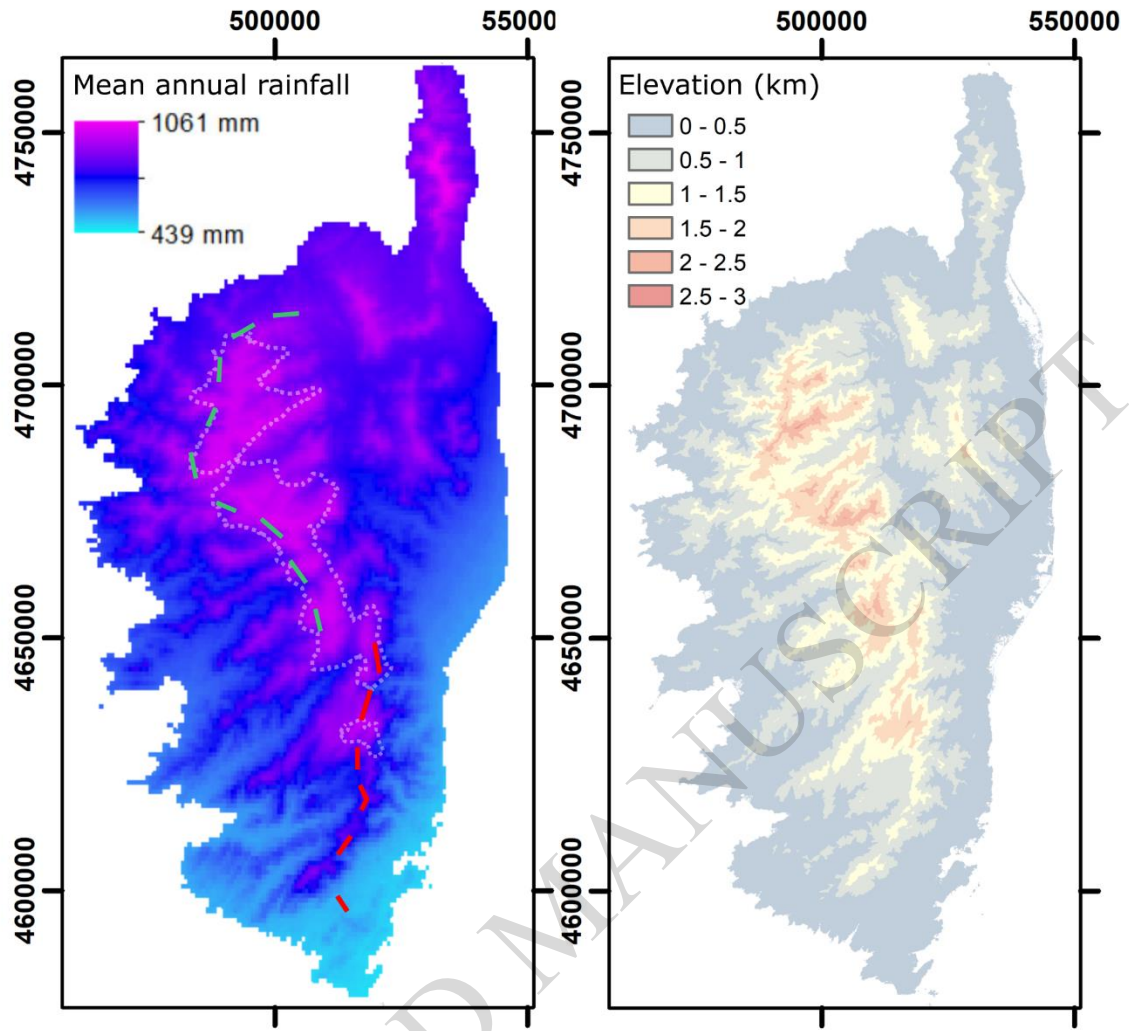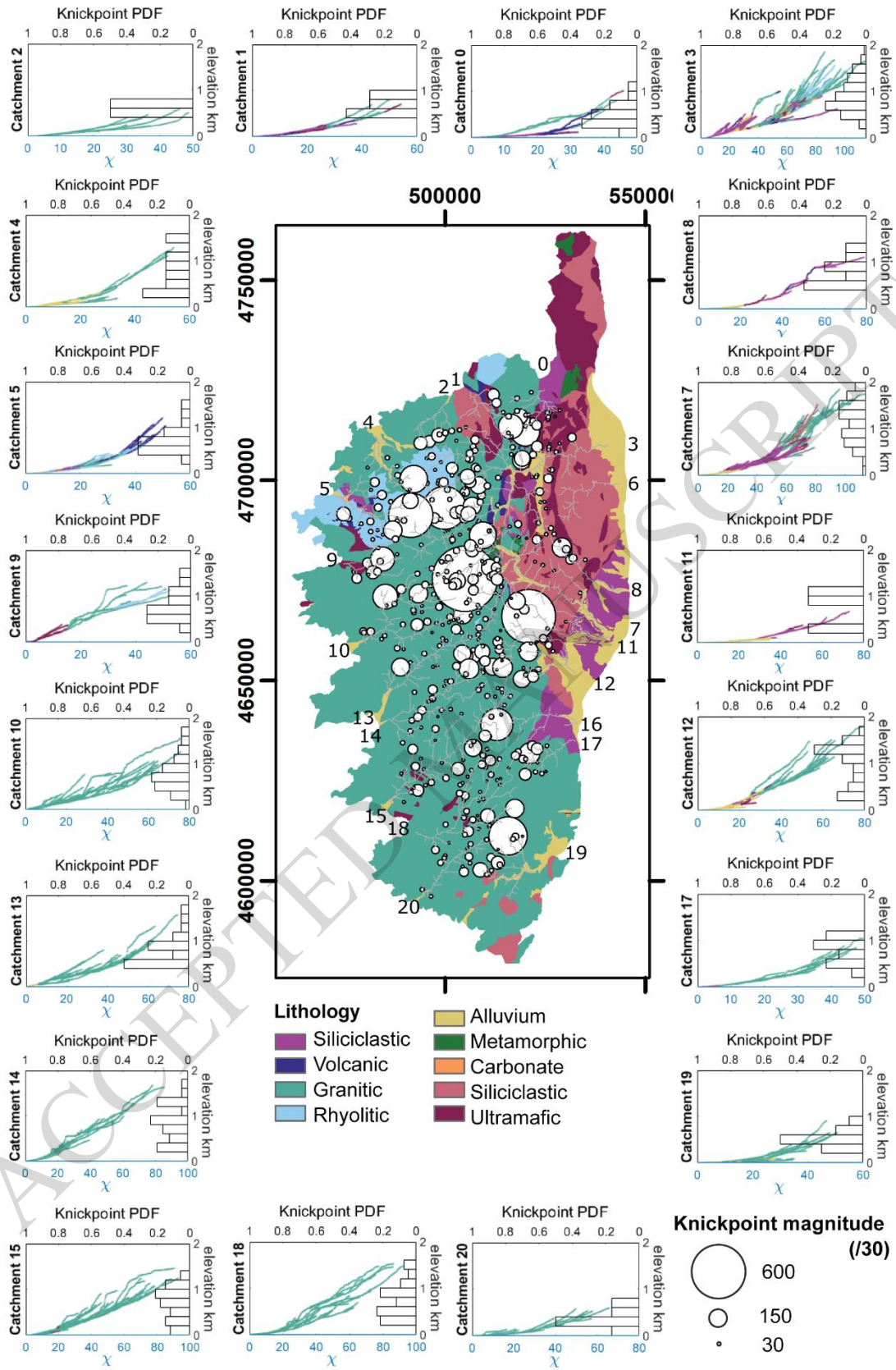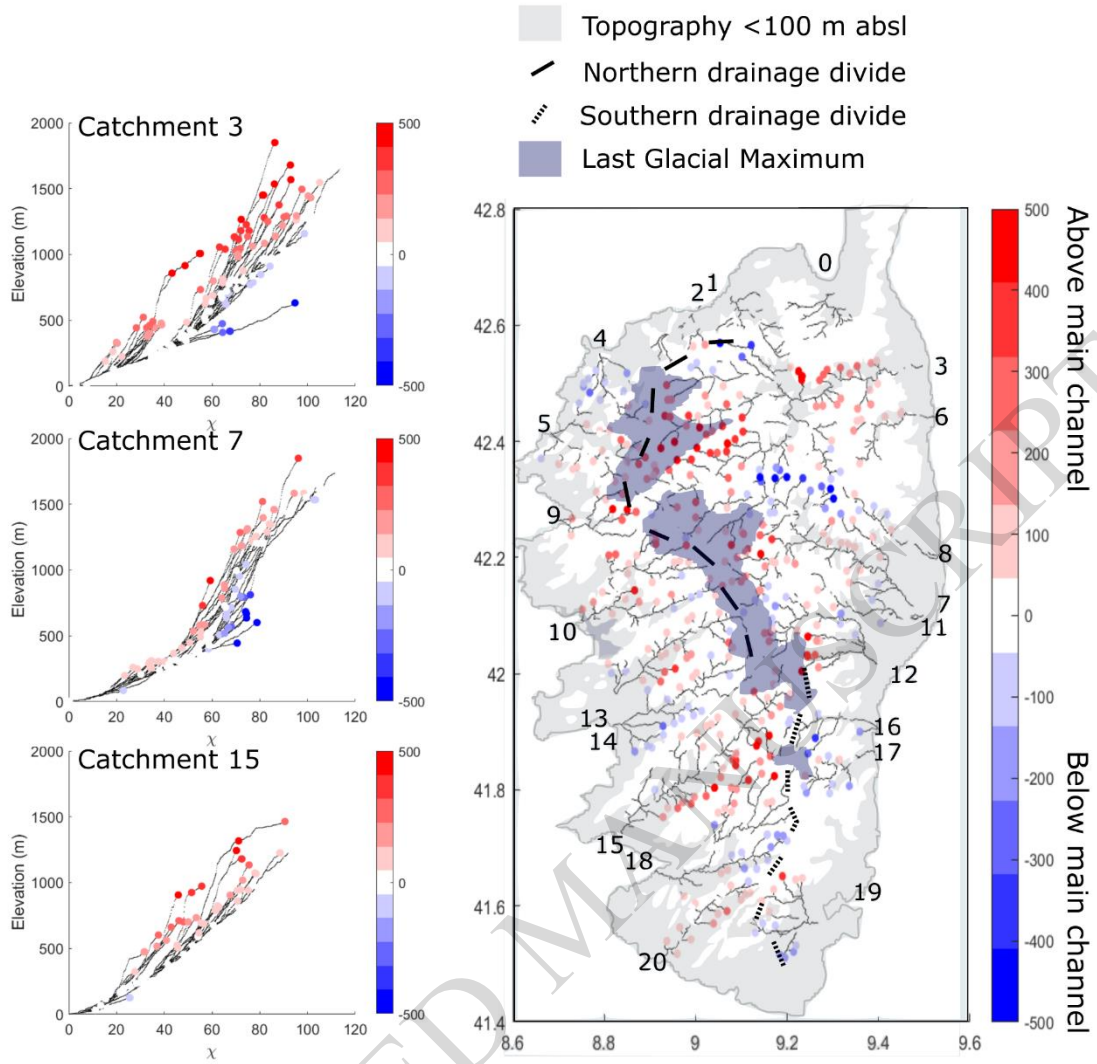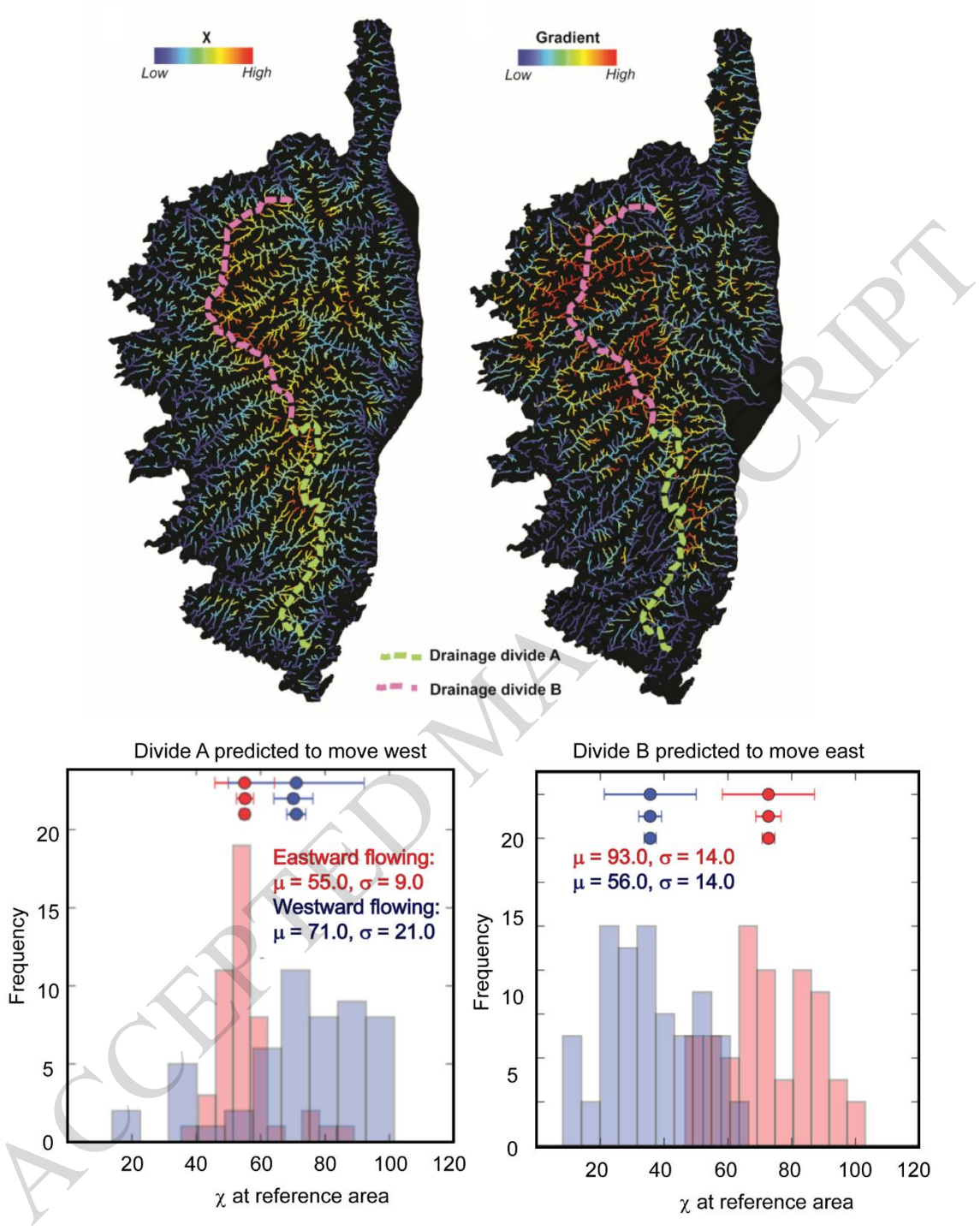
Figure 1

Figure 2

Figure 3

Figure 4

Figure 5